

**To cite this article:** YUE X S, ZHOU H, KONG X S, et al. Experimental and simulation study of afterburning effect for blast load in confined cabin[J/OL]. Chinese Journal of Ship Research, 2023, 18(4). <http://www.ship-research.com/en/article/doi/10.19693/j.issn.1673-3185.02708>.

**DOI:** 10.19693/j.issn.1673-3185.02708

# Experimental and simulation study of afterburning effect for blast load in confined cabin



YUE Xuesen<sup>1</sup>, ZHOU Hu<sup>1</sup>, KONG Xiangshao<sup>\*2</sup>, ZHENG Cheng<sup>2</sup>, WU Weiguo<sup>2</sup>

1 School of Naval Architecture, Ocean and Energy Power Engineering, Wuhan University of Technology, Wuhan 430063, China

2 Green & Smart River-Sea-Going Ship, Cruise and Yacht Research Center, Wuhan University of Technology, Wuhan 430063, China

**Abstract:** [Objectives] The afterburning effect need to be considered when TNT explodes inside a confined space. In order to accurately analyze the internal blast load, it is necessary to explore the relationship between the afterburning energy value and the charge volume ratio. [Methods] The explosion experiments of 5 different masses of TNT were performed in the confined spaces filled with air and helium. Based on three different methods of chemical reaction analysis, energy conservation law and hypothetical isentropic process, the corresponding afterburning energy of five different charge volume ratios is calculated. The numerical simulation of explosion in confined space considering afterburning effect was realized by ANSYS/AUTODYN program. [Results] The comparison between quasi-static pressure simulation results and experimental results shows that the theoretical value of afterburning energy calculated by chemical reaction analysis method can only be used as the upper limit value, the accuracy of energy conservation method depends on the adiabatic index of mixed gas, and the error of assumed isentropic process method is stable between 4%–7%. Different afterburning energy release processes do not change the final quasi-static pressure, but only the reflected shock wave pressure. [Conclusions] The research results can provide more accurate input load for the design and damage assessment of anti-explosion structures.

**Key words:** internal blast load; afterburning effect; energy release; quasi-static pressure

**CLC number:** U661.4; O383<sup>+.3</sup>

## 0 Introduction

Large surface vessels, due to their immense strategic significance and substantial size, have emerged as the primary focal points for anti-ship missile attacks. Among the various threats they face, the damage caused by penetrating explosions presents a particularly grave danger to the survival of such vessels. According to statistics, more than 20 ships in China and abroad have been damaged or sunk by anti-ship missiles in actual combat or target practice since the 1960s<sup>[1]</sup>. When explosions occur

inside the cabins of ships, the form and evolution of the blast loads differ significantly from those in the case of explosions in open spaces since the confined environment exerts a notable influence on the explosion loads<sup>[2]</sup>. In addition to the initial shock wave, the combustion of detonation products significantly enhances subsequent reflected shock waves and quasi-static pressures during the explosion. Accurate and reliable analysis of explosion loads within cabins plays a crucial role in the structural protection design and damage assessment of ships.

**Received:** 2021 – 12 – 14

**Accepted:** 2022 – 01 – 13

**Supported by:** National Natural Science Foundation of China (52171318)

**Authors:** YUE Xuesen, male, born in 1997, master degree. Research interest: Ship blast and impact resistance.

E-mail: yuexs@whut.edu.cn

KONG Xiangshao, male, born in 1983, Ph.D., professor. Research interest: Ship explosion damage and protection.

E-mail: kongxs@whut.edu.cn

**\*Corresponding author:** KONG Xiangshao

Scholars in China and abroad have conducted a series of experiments and numerical simulations to study the afterburning effect on explosions in confined spaces. Researcher Ornellas<sup>[3]</sup> at the Lawrence Livermore National Laboratory in the United States was among the first to experimentally demonstrate the existence of the afterburning effect. In the experiment, he detonated 25 g of TNT inside a 5.3 L spherical container and measured the heat released during the explosion in a vacuum environment and in an oxygen environment, respectively. He observed that the total energy released when the explosion occurred in an oxygen environment was higher than that in a vacuum environment. Following Ornellas' approach, a number of researchers<sup>[4-8]</sup> adjusted the oxygen content of the air in confined containers and compared the quasi-static pressure after explosives detonate in different gas environments. Ultimately, they all reached the same conclusion: the additional energy released by the combustion reaction of detonation products enhanced the internal blast load to an extent that shall not be ignored. In the realm of theoretical research, scholars such as Edri et al.<sup>[9-10]</sup>, Wang et al.<sup>[5]</sup>, Zhong et al.<sup>[11]</sup>, Xu et al.<sup>[12]</sup>, and Li et al.<sup>[13]</sup> have each developed theoretical quasi-static pressure calculation models considering the afterburning effect on the basis of the thermodynamic relationships between energy and pressure. They also provided the relationships between the quasi-static pressure and the charge-to-volume ratio. Regarding numerical simulation-based studies of the afterburning effect, Kuhl et al.<sup>[14]</sup> conducted extensive work in this aspect using self-developed programs to investigate the kinetics of the multi-component chemical reactions of detonation products, combustion models, and turbulence effects. Furthermore, several scholars abroad have also conducted a numerical simulation-based study of the combustion process of the afterburning effect with self-developed programs<sup>[15-18]</sup>. Similarly, Chinese scholars Xu et al.<sup>[19-21]</sup> coupled a simplified reaction rate model into three-dimensional two-component compressible Euler equations and added combustion energy in the form of a source term to approximate the afterburning effect. Li et al.<sup>[22]</sup> numerically simulated the energy release patterns when thermobaric explosives detonated in confined containers with a gas-solid two-phase reaction flow model. In the aspect of general finite-element software, Xin et al.<sup>[23]</sup> were

among the first to implement numerical simulations of TNT explosions in the air considering the afterburning effect using the software AUTODYN. Afterward, Edri et al.<sup>[24]</sup>, Cao et al.<sup>[25]</sup>, Hernandez et al.<sup>[26]</sup>, and Kong et al.<sup>[27]</sup> proposed various numerical simulation methods that gave due consideration to combustion energy using the AUTODYN platform.

A summary of the current state of the research in China and abroad mentioned above indicates that experimental studies of the afterburning effect are still unable to directly capture the release energy process of the afterburning effect. Instead, they can only assess the enhancement effect of the process according to the final quasi-static pressure and are limited to specific experimental conditions. Therefore, numerical simulation remains an effective approach for investigating internal blast loads. Currently, numerical simulation-based studies of the afterburning effect can be divided into two categories. One involves the in-depth discussion of the combustion process with self-developed numerical programs from perspectives such as fluid dynamics and the kinetics of multi-component chemical reactions. Focusing primarily on exploring combustion mechanisms, such an approach entails a substantial amount of computational work and is currently inapplicable to general finite-element software. Additionally, the complexity of the models introduces significant uncertainty to the results. The other category involves simulations with the simplified combustion energy release models provided by general finite-element software. However, this approach often lacks a clear explanation of the rationale behind the addition of combustion energy. The simplified simulation methods provided by general finite-element software do not rely on complex physical models. They can simulate explosion loads as accurately as complex methods if appropriate values of combustion energy are added and reasonable energy release rates are provided.

To address these issues, the authors of this study will conduct comparative experiments on TNT explosion loads in confined spaces providing air and helium environments. The authors conclude three calculation methods for combustion energy from the previous research. Furthermore, the software ANSYS/AUTODYN will be used to numerically simulate the processes of TNT

explosions in confined spaces. The simulation results will be compared with experimental data to assess the accuracy of the calculation methods. Common military single-compound explosives are typically explosives with negative oxygen balance. The authors take TNT as an example for the study, and the research methods employed are also applicable to other CHON explosives.

## 1 Experiments and results

### 1.1 Experimental conditions

In this aspect, experiments were conducted to study the explosion of TNT within a confined space. The experimental setup consisted of a self-designed square explosion chamber (Fig. 1) with internal dimensions of 400 mm×400 mm×900 mm. A TNT column was suspended at the center of the explosion chamber, with its axis perpendicular to the B-side. The initiation point was located above the TNT column, and electric detonators were used for initiation. The experimental conditions are outlined in Table 1, with a focus on two variables, namely, the charge and the gas environment. Several wall pressure sensors designated as P1 were positioned on the A-, B-, and C-side of the explosion chamber to measure the internal pressure. The coordinates of the pressure measurement point relative to the center of the explosion chamber were (-200, -225, 38). Reference [8] is available for more detailed information on the experimental scheme.

### 1.2 Experimental results and analysis

The typical time-history curves of the pressure measured during the experiments are shown in Fig. 2. After fluctuating for 5–10 ms, the shockwave pressure gradually stabilizes and eventually reaches a quasi-static state. In this study, the pressure in the

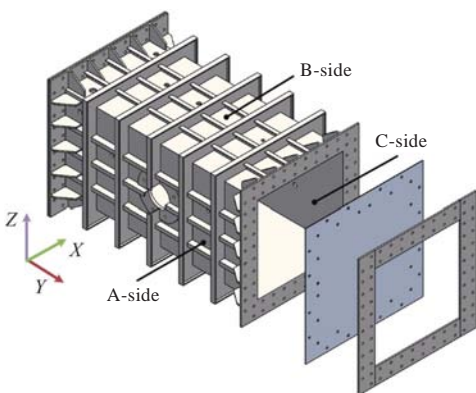


Fig. 1 Experimental setup for explosions

Table 1 Experimental conditions

Condition No.	Charge/g	Gas environment	TNT column diameter/mm
1	7.50	Air (oxygen content: 2.1%)	20
2	11.25		20
3	15.00		25
4	22.50		25
5	30.00		30
6	7.50	Helium (oxygen content: 2.2%)	20
7	11.25		20
8	15.00		25
9	22.50		25
10	30.00		30

steady state was averaged to serve as the quasi-static pressure at the measurement point. The quasi-static pressure results obtained under the various experimental conditions are summarized in Table 2. In the experiments, the pressure measured using pressure sensors is gauge pressure, while that obtained through theoretical derivation and numerical simulations is absolute pressure. To avoid any confusion, the authors uniformly describe pressure as absolute pressure and add atmospheric pressure to the pressure measured during the experiments for correction.

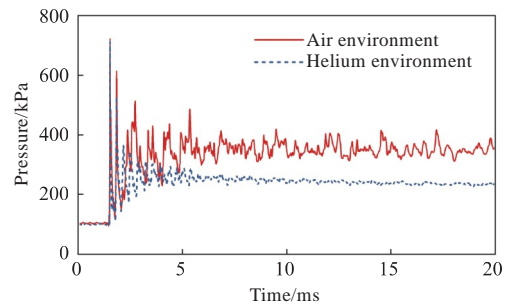


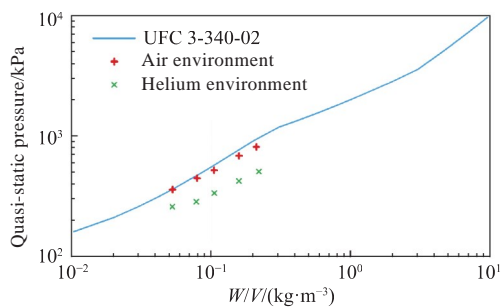
Fig. 2 Time-history curves of pressure at measurement point P1 in the case of a charge of 7.50 g

A comparison of the measurement results in Table 2 reveals that the quasi-static pressure in the cases of TNT explosions in an air environment is 100 to 307 kPa higher than that in a helium environment, representing a percentage increase of 38% to 62%. It indicates that the afterburning effect of the detonation products generated by TNT explosions under aerobic conditions significantly affects the explosion loads in a confined space. Moreover, the degree of influence varies considerably with the charge. Consequently, only qualitative conclusions can be drawn from a limited number of experimental results.

**Table 2 Comparison of quasi-static pressure under different conditions**

Charge/g	Quasi-static pressure/kPa		Increase/kPa	Percentage increase/%
	Air environment	Helium environment		
7.50	360	260	100	38
11.25	448	286	162	57
15.00	521	337	184	55
22.50	690	425	265	62
30.00	817	510	307	60

The relationship between the quasi-static pressure and the charge-to-volume ratio ( $W/V$ ), where  $W$  is the mass of the explosive and  $V$  is the volume of the confined space, is depicted in Fig. 3. Additionally, the results obtained from a significant number of experiments in the Unified Facilities Criteria (UFC) 3-340-02 (hereinafter shortened to UFC) issued by the U.S. Department of Defense [28] are also plotted in the figure. Clearly, the quasi-static pressure obtained under air conditions aligns well with the UFC results, which affirms the reliability of the experiments conducted in this study. Furthermore, since the UFC also provides quasi-static pressure values corresponding to a wide range of the charge-to-volume ratio ( $W/V$ ), it can serve as a reference for the subsequent calculation of the combustion energy corresponding to any  $W/V$ .

Fig. 3 Relationship between quasi-static pressure and  $W/V$ 

## 2 Calculation methods for combustion energy of detonation products

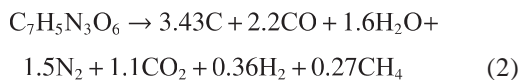
The energy released during the explosion per unit mass of an explosive in a confined space is denoted as  $Q$  and can be divided into two components: one is the energy released from the detonation reaction, known as the detonation heat ( $Q_e$ ), and the other is the energy released from the combustion of combustible detonation products ( $Q_{ab}$ ). This relationship can be expressed as:

$$Q = Q_e + Q_{ab} \quad (1)$$

The detonation heat ( $Q_e$ ) can be determined through detonation calorimetry as specified in GJB 772A-1997 "Test Methods for Explosives." In this method, the explosive is detonated in an oxygen-free environment within a calorimeter, and the measured explosion energy is considered the detonation heat. The detonation heat of a given explosive is considered constant but influenced by the charge density. Typically, a higher charge density of the explosive leads to a slight increase in the detonation heat [29, 30]. The combustion energy ( $Q_{ab}$ ) depends on the oxygen content in the confined space and varies with the charge-to-volume ratio ( $W/V$ ). Therefore, determining the combustion energy  $Q_{ab}$  corresponding to any charge-to-volume ratio  $W/V$  is particularly important. In the following part, three calculation methods for combustion energy will be presented by taking TNT as an example.

### 2.1 Method 1 based on chemical reactions

The chemical reaction during TNT detonation is as follows [17]:



The detonation heat of TNT is calculated to be 4.47 MJ/kg from the above chemical reaction equation by applying Hess's law. Additionally, detonation products, such as C, CO,  $\text{H}_2$ , and  $\text{CH}_4$ , can further undergo the combustion reactions in Table 3. Theoretically, the complete combustion of the detonation products generated from 1 kg of TNT requires 2.58  $\text{m}^3$  of air. On this basis, the critical  $W/V$  differentiating complete combustion from partial combustion is determined to be 0.387  $\text{kg}/\text{m}^3$ . When  $W/V$  is smaller than 0.387  $\text{kg}/\text{m}^3$ , the detonation products are assumed to have undergone complete combustion. According to Table 3, the maximum combustion energy of the detonation products of TNT can be calculated to be 10.01 MJ/kg. When  $W/V$  is larger than 0.387  $\text{kg}/\text{m}^3$ , an assumption is made that the oxygen in the confined space is insufficient and that the detonation products undergo incomplete combustion. The combustion energy  $Q_{ab}$  calculated on the basis of chemical reactions can be expressed as Eq. (3):

$$Q_{ab} = \begin{cases} Q_{ab\_max}, & W/V \leq 0.387 \text{ kg/m}^3 \\ \frac{V}{W \cdot \Gamma} \cdot Q_{ab\_max}, & W/V \geq 0.387 \text{ kg/m}^3 \end{cases} \quad (3)$$

where  $Q_{ab\_max} = 10.01 \text{ MJ/kg}$ ;  $\Gamma = 2.58 \text{ m}^3/\text{kg}$



**Table 3 Combustion reactions and combustion heat**

Combustion reaction	Combustion heat/(kJ·mol <sup>-1</sup> )
C + O <sub>2</sub> → CO <sub>2</sub>	393.6
CO + 0.5O <sub>2</sub> → CO <sub>2</sub>	282.8
H <sub>2</sub> + 0.5O <sub>2</sub> → H <sub>2</sub> O	241.8
CH <sub>4</sub> + 2O <sub>2</sub> → CO <sub>2</sub> + 2H <sub>2</sub> O	800.0

## 2.2 Method 2 based on energy conservation

The ideal gas law can be written in the following form:

$$p = \rho(\gamma - 1)e \quad (4)$$

where  $p$  is the gas pressure;  $\rho$  is the gas density;  $\gamma$  is the adiabatic index of the gas;  $e$  is the internal energy per unit mass of the gas. According to Eq. (4), the internal energy  $E$  of a gas with a volume  $V$  in a confined space can be expressed as

$$E = \frac{p}{\rho(\gamma - 1)} \cdot \rho V \quad (5)$$

In the case of TNT explosions in a confined space, the energy losses caused by heat transfer and deformation are temporarily left aside, and the post-explosion mixed gas is assumed to satisfy the ideal gas law. Then, the following equation can be derived from the energy conservation relationship [10]:

$$\frac{p_0}{\rho_0(\gamma_0 - 1)} \rho_0 (V - V_E) + Q \rho_E V_E = \frac{p_m}{\rho_m(\gamma_m - 1)} \rho_m V \quad (6)$$

where  $p_0 = 101.3$  kPa (the initial air pressure);  $\rho_0$  is the initial air density;  $\gamma_0$  is the adiabatic index of air and is set to 1.4;  $V$  is the volume of the confined space;  $V_E$  is the volume of the explosive;  $\rho_E$  is the density of the explosive;  $Q$  is the energy released per unit mass of the explosive;  $p_m$  is the quasi-static pressure of the mixed gas after the explosion;  $\gamma_m$  is the adiabatic index of the mixed gas;  $\rho_m$  is the density of the mixed gas. The first term on the left side of Eq. (6) is the internal energy of the air in the confined space, while the second term is the internal energy of the explosive. Moreover, the right side of the equation is the total energy within the system after the explosion.

The expression of  $Q$  can be obtained by substituting  $W = \rho_E V_E$  into Eq. (6) and rewriting it:

$$Q = \frac{p_0}{\rho_E(\gamma_0 - 1)} + \left( \frac{p_m}{\gamma_m - 1} - \frac{p_0}{\gamma_0 - 1} \right) \frac{W}{V} \quad (7)$$

In Eq. (7), the energy  $Q$  released per unit mass of the explosive is expressed as a function of the charge-to-volume ratio  $W/V$ , the quasi-static pressure  $p_m$  of the mixed gas, and the adiabatic index  $\gamma_m$  of the mixed gas. The adiabatic index of

the mixed gas is also related to the charge-to-volume ratio  $W/V$ , and this relationship is provided in Reference [10] and shown in Fig. 4. Additionally, Fig. 3 provides the relationship between the quasi-static pressure and the charge-to-volume ratio. Therefore, the energy  $Q$  released per unit mass of the explosive corresponding to any charge-to-volume ratio  $W/V$  can be calculated from Eq. (7) with the experimentally measured quasi-static pressure.

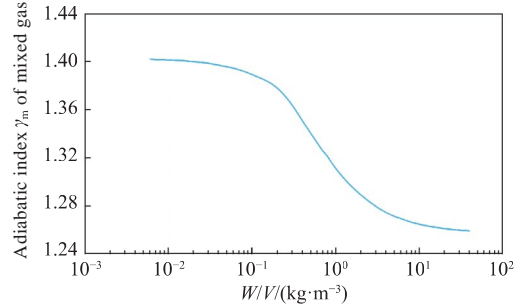


Fig. 4 Variation in adiabatic index with  $W/V$

## 2.3 Method 3 based on isentropic process assumption

When the Jones-Wilkins-Lee (JWL) state equation is used to simulate TNT explosions during numerical calculations, TNT and air are considered independent and described by respective gas state equations. Due to this characteristic, a combustion energy calculation method was proposed in Reference [26]. This method involves three important points: One is that it needs the numerical simulation results obtained without considering combustion energy; then, it requires a known quasi-static pressure obtained with due consideration to the afterburning effect, and this pressure can generally be obtained by experiments or by referring to the UFC curves in Fig. 3; last but not least, it divides the explosion process into detonation and combustion, which are discussed separately, and assumes that the energy release during combustion is an isentropic process.

As shown in Fig. 5, an explosion of TNT in a confined space is simplified into three states: State 0 is the initial state when TNT has not been detonated; State 1 is the final quasi-static state in the absence of combustion energy; State 2 is the final quasi-static state in the presence of combustion energy. The transition from State 0 to State 1 is the detonation process, which involves the propagation and reflection of detonation waves and is a non-isentropic process. The transition from

State 1 to State 2 is the combustion process, which is relatively stable and slow compared with the detonation process and can be considered an isentropic process. Then, the transition of air from State 1 to State 2 in Fig. 5 is an isentropic compression process and thus satisfies the following thermodynamic relationship:

$$p_1 \cdot (V_{\text{air}_1})^{\gamma_{\text{air}}} = p_2 \cdot (V_{\text{air}_2})^{\gamma_{\text{air}}} \quad (8)$$

where  $p_1$  is the quasi-static pressure in the absence of combustion energy;  $V_{\text{air}_1}$  is the volume of air in the quasi-static state in the absence of combustion energy;  $p_2$  is the quasi-static pressure in the presence of combustion energy;  $V_{\text{air}_2}$  is the volume of air in the quasi-static state in the presence of combustion energy;  $\gamma_{\text{air}}$  is the adiabatic index of air and is set to 1.4. Noteworthy, Eq. (8) is only applicable to air and does not apply to the explosion products of TNT since an isentropic process

requires adiabatic reversibility, but the expansion of the detonation products of TNT is non-isentropic due to the energy absorption during the expansion. Furthermore, the air pressure, the gas pressure from the detonation products of TNT, and the overall pressure in the confined system are equal. The values of state variables  $p_1$  and  $V_{\text{air}_1}$  corresponding to State 1 can be obtained through numerical simulation without considering combustion energy, and the quasi-static pressure  $p_2$  corresponding to State 2 is set to its experimental value. On this basis, Eq. (8) can be used to calculate the volume of air  $V_{\text{air}_2}$  in the quasi-static state in the presence of combustion energy. Additionally, volume conservation can be expressed as follows:

$$V_{\text{air}_2} + V_{\text{TNT}_2} = V_{\text{total}} \quad (9)$$

Mass conservation can be presented as the following equation:

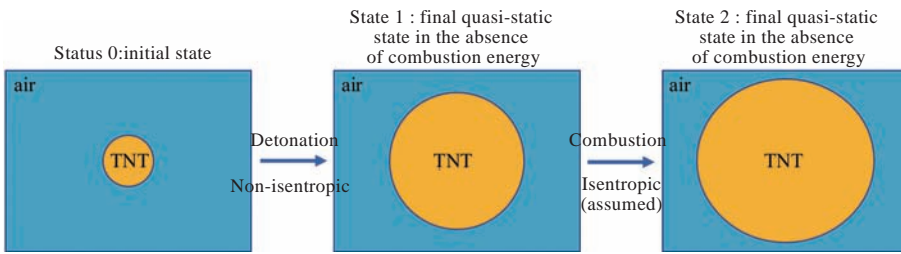


Fig. 5 Process of TNT explosion in confined space

$$\begin{aligned} m_{\text{air}} &= \rho_{\text{air}_2} V_{\text{air}_2} \\ m_{\text{TNT}} &= \rho_{\text{TNT}_2} V_{\text{TNT}_2} \end{aligned} \quad (10)$$

The state equation can be written as

$$\begin{aligned} p_2 &= \rho_{\text{air}_2} (\gamma_{\text{air}} - 1) e_{\text{air}_2} \\ p_2 &= \rho_{\text{TNT}_2} (\gamma_{\text{TNT}} - 1) e_{\text{TNT}_2} \end{aligned} \quad (11)$$

Energy conservation can be described as follows:

$$(Q_e + Q_{\text{ab}})m_{\text{TNT}} + e_{\text{air}_0}m_{\text{air}} = e_{\text{TNT}_2}m_{\text{TNT}} + e_{\text{air}_2}m_{\text{air}} \quad (12)$$

The combustion energy  $Q_{\text{ab}}$  can be obtained by solving Eqs. (8) to (12) sequentially.

Fig. 6 presents the relationship between the combustion energy  $Q_{\text{ab}}$  calculated by the above three methods and the charge-to-volume ratio  $W/V$ . In the calculations, the detonation heat  $Q_e$  is uniformly set to 4.47 MJ/kg, and the experimental

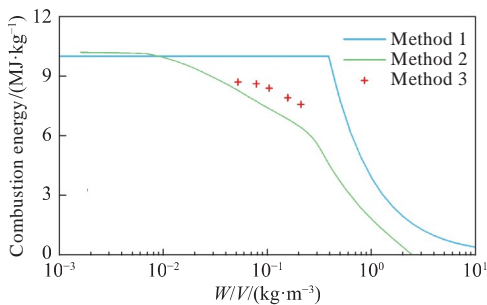


Fig. 6 Relationship between combustion energy and  $W/V$

data used in methods 2 and 3 are taken from the UFC curves in Fig. 3. Since the calculation process of Method 3 is relatively complex, only five typical values are calculated for comparison.

### 3 Numerical simulation of enhancement effect of combustion on explosions in confined spaces

The finite-element software ANSYS/AUTODYN was utilized to numerically simulate the experimental conditions described in Section 1. The enhancement effect of combustion was examined by adding additional energy to the JWL state equation. A three-dimensional (3D) multi-material Eulerian algorithm was used to solve the process of explosions in confined spaces.

#### 3.1 Finite-element model

The air domain model is shown in Fig. 7, with dimensions of 400 mm × 400 mm × 900 mm. It was simulated using multi-material Eulerian elements, and the mesh size was set to 5 mm after

convergence analysis of the mesh size. The square explosion chamber can be considered a rigid body since it does not deform within the design charge range. Comparative calculation further reveals that the change in the volume of the internal space and the energy absorbed due to the deformation of the square end plate have little effect on the final quasi-static pressure. Therefore, the structural response is temporarily left aside during the simulation. In the experiments, the energy of the detonators was measured in 1 g TNT equivalent. In the simulations, the TNT charge was set to be 1 g higher than the nominal charge specified in the experimental conditions. The spatial distribution of the pressure load from the shock waves generated by the explosive column is axially symmetric. Therefore, the pressure load from the shock waves can be calculated by mapping it to the 3D space using its 2D axial symmetry. The mesh size for the 2D calculations was set to 0.5mm. Noteworthy, the 2D calculations should be terminated before the shock wave pressure reaches the sides of the chamber. This approach ensures both high calculation accuracy and high calculation efficiency.

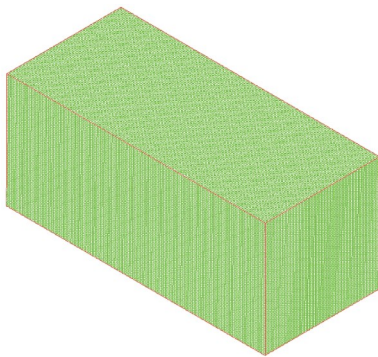


Fig. 7 Air domain model

Air was described using the ideal gas law, and its expression was similar to Eq. (4). The corresponding parameters were set as follows:  $\rho=1.225 \text{ kg/m}^3$ ;  $\gamma = 1.4$ ;  $e = 2.068 \times 10^5 \text{ J/kg}$ .

A JWL equation as shown in Eq. (13) was adopted as the state equation for TNT:

$$p = A \left( 1 - \frac{w\eta}{R_1} \right) e^{-\frac{R_1}{\eta}} + B \left( 1 - \frac{w\eta}{R_2} \right) e^{-\frac{R_2}{\eta}} + wpe \quad (13)$$

where  $p$  is the pressure of the detonation products.  $A, B, R_1, R_2,$  and  $w$  are constants.  $\eta = \rho/\rho_0$ ;  $\rho$  is the density of the detonation products.  $\rho_0$  is the reference density, namely, the initial charge density of TNT;  $e$  is the internal energy per unit mass of the detonation products, with its initial value set to the detonation heat ( $e_0=Q_e$ ). The material parameters of

TNT are selected by referring to Reference [29] and are listed in Table 4.

Table 4 Parameters of JWL state equation for explosive TNT

$\rho/\text{g}\cdot\text{cm}^{-3}$	$A/\text{GPa}$	$B/\text{GPa}$	$R_1$	$R_2$	$w$	$e_0/(\text{MJ}\cdot\text{m}^{-3})$
1.55	307	3.9	4.485	0.79	0.3	6 495

The five parameters  $A, B, R_1, R_2,$  and  $w$  in the JWL state equation are determined by fitting using the kinetic data measured through standard cylinder tests on the premise of known initial charge density ( $\rho_0$ ), detonation velocity ( $D$ ), adiabatic index ( $\gamma$ ), and detonation heat ( $Q_e$ ) of the explosive. The detonation heat ( $Q_e$ ) is generally measured in an oxygen-free environment. During cylinder tests, the explosive cannot fully interact with the air. Therefore, for explosives with negative oxygen balance, the parameters of the JWL state equation have certain limitations as they do not take into account the energy released by the combustion of the detonation products. Hence, they need to be corrected in simulation calculations by adding additional energy. This functionality can be fulfilled by general finite-element programs such as AUTODYN and LS-DYNA. In this study, the combustion energy in the cases of explosions of five different charges of the explosive in an air environment was calculated by the three methods described in Section 2, with the results listed in Table 5.

Table 5 Combustion energy corresponding to different charges

Charge/g	Detonation heat <sup>[29)]/(MJ·kg<sup>-1</sup>)</sup>	Combustion energy/(MJ·kg <sup>-1</sup> )		
		Method 1	Method 2	Method 3
7.50	4.190	10.010	8.449	8.895
11.25	4.190	10.010	7.207	7.928
15.00	4.190	10.010	6.267	7.109
22.50	4.190	10.010	5.741	6.531
30.00	4.190	10.010	5.005	5.824

### 3.2 Comparison of simulation results with experimental results

The quasi-static pressure is a critical damage mechanism in the cases of explosions in confined spaces and also describes the characteristics of combustion energy release. In this study, the quasi-static pressure was used as an indicator to quantitatively analyze the simulation results. Table 6 and Fig. 8 both compare the quasi-static pressure

**Table 6** Error between simulated and experimental quasi-static pressure

Charge/g	Experimental value/kPa	Simulated value					
		Method 1/kPa	Error/%	Method 2/kPa	Error/%	Method 3/kPa	Error/%
7.50	360	365	1.4	339	-5.8	345	-4.1
11.25	448	467	4.3	404	-9.7	420	-6.2
15.00	521	578	11.0	468	-10.2	491	-5.7
22.50	690	810	17.4	619	-10.3	653	-5.3
30.00	817	1028	25.9	737	-9.7	778	-4.7

obtained from experiments with that obtained from simulations by different calculation methods for combustion energy.

The error among the simulation calculation results of the quasi-static pressure obtained by Method 1 and the experimental data ranges from 1% to 26% and is invariably positive. Moreover, it gradually increases with the charge. Method 1 only pays attention to the oxygen content when it is employed to calculate the combustion energy on the basis of the chemical reactions. When  $W/V$  is smaller than  $0.387 \text{ kg/m}^3$ , the combustion energy will always be  $10.01 \text{ MJ/kg}$ . In reality, however, whether the combustion of the detonation products is complete depends not only on the oxygen content but also on whether they come into full contact with oxygen. In the experiment in Reference [6],  $100 \text{ g}$  of TNT was detonated in a  $0.5 \text{ m}^3$  confined container. Consequently, the quasi-static pressure was  $240 \text{ MPa}$  in an air environment and  $289 \text{ MPa}$  in a pure oxygen environment. This condition corresponded to a  $W/V$  of  $0.2 \text{ kg/m}^3$ , which was below the theoretical critical value  $0.387 \text{ kg/m}^3$ . This indicates that although the oxygen content in the air environment theoretically meets the requirements, the combustion energy is not entirely released. In other words, when TNT detonates in an air environment, the actual critical value of  $W/V$  determining the complete release of combustion energy is smaller than the theoretical value  $0.387 \text{ kg/m}^3$ . A reference to Fig. 6 reveals that the

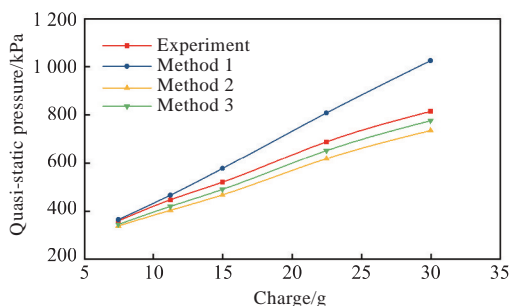


Fig. 8 Comparison of simulation results with experimental results

combustion energy calculated by Method 1 is higher than the actual value. Nevertheless, it can serve as an upper limit and is thus still of important reference value.

The error among the simulation calculation results of the quasi-static pressure obtained by Method 2 and the experimental data ranges from 5% to 11% and is invariably negative. The error in Method 2 is mainly related to the setting of the adiabatic index  $\gamma_m$  of the post-explosion mixed gas in Eq. (7). Sensitivity analysis reveals that the energy  $Q$  released by the explosive in Eq. (7) is highly sensitive to  $\gamma_m$ . The setting of  $\gamma_m$  significantly affects the magnitude of the combustion energy. The value of  $\gamma_m$  used by Method 2 when calculating the combustion energy from Eq. (7) is shown in Fig. 4. This value is a theoretical value derived through chemical reaction analysis. However, in the finite-element program AUTODYN, the  $\gamma$  of air remains 1.4, and that of the detonation products of TNT remains 1.3. Table 7 provides two sets of simulation results corresponding to different  $\gamma_m$ . The  $\gamma_m$  for Set 1 is taken from Fig. 4. In contrast, the one for Set 2 is the equivalent  $\gamma_m$  calculated from Eq. (14) using the air volume  $V_{\text{air-1}}$  and the volume  $V_{\text{TNT-1}}$  of the detonation products of TNT when the quasi-static pressure is obtained by simulation calculation with no consideration given to the combustion energy.

$$\frac{V_{\text{air-1}}}{\gamma_{\text{air}} - 1} + \frac{V_{\text{TNT-1}}}{\gamma_{\text{TNT}} - 1} = \frac{V_{\text{total}}}{\gamma_m - 1} \quad (14)$$

According to Table 7, even small variations in  $\gamma_m$  can result in significant differences in the final results. The error corresponding to the  $\gamma_m$  for Set 2 is smaller than 3%, indicating that the improved Method 2 has a smaller error. This result also underscores the importance of determining a reliable  $\gamma_m$  value to ensure the accuracy of Method 2.

Among the three calculation methods, Method 3 is the one whose results best match the experimental values. Its error ranges from 4% to



**Table 7 Comparison of results corresponding to different adiabatic indexes obtained by Method 2**

	Charge/g	Adiabatic index $\gamma_m$	Combustion energy $Q_{ab}/(\text{MJ}\cdot\text{kg}^{-1})$	Simulated quasi-static pressure/kPa	Error between simulated and experimental values/%
Set 1	7.50	1.395	8.449	339	-5.8
	11.25	1.392	7.207	404	-9.7
	15.00	1.388	6.267	468	-10.2
	22.50	1.382	5.741	619	-10.3
	30.00	1.377	5.005	737	-9.7
Set 2	7.50	1.354	10.474	373	3.7
	11.25	1.350	8.929	441	-1.5
	15.00	1.348	7.739	511	-1.9
	22.50	1.345	6.981	673	-2.4
	30.00	1.344	5.988	793	-2.9

7% and is invariably negative. As mentioned above, the error in Method 2 can be attributed to the uncertainty in  $\gamma_m$ . To address this issue, Method 3 examines air and TNT separately and assumes that the air in the absence of the combustion energy and that in the presence of the combustion energy both meet the conditions of isentropic compression. This approach leads to Eq. (8), where  $\gamma_{\text{air}}$  is constant. The combustion energy can then be calculated by referring to the experimental data and the conservation relationships. Avoiding the uncertainty of  $\gamma_m$ , Method 3 keeps the error in the final results at around 5%. Its error can partly be attributed to the fact that the isentropic process assumption is an ideal case. In practice, however, this process is only approximately isentropic and is thus not genuinely isentropic. Additionally, the energy is not strictly conserved when AUTODYN is employed to solve explosion problems. An analysis of the energy conservation curve during the simulation calculation process reveals that the total energy decreases to varying degrees during the combustion energy release under different conditions, leading to comparatively small numerical calculation results.

## 4 Effect of energy release history on pressure

The afterburning effect on explosions in confined spaces has two key aspects: the magnitude of energy release and the energy release history. In AUTODYN, the addition of additional energy prerequisites not only the determination of the value of combustion energy  $Q_{ab}$  but also the definition of the start time ( $t_0$ ) and end time ( $t_1$ ) of energy release. In the numerical simulation calculation conducted in Section 3, the  $t_0$  and  $t_1$  were set to 0.2

and 1 ms, respectively. Specifically, the peak overpressure of the shock wave occurs approximately at 0.2 ms, and this observation serves as the basis for determining the start time of energy release. Additionally, the shock wave reflects after it reaches the sides, leading to multiple peaks of the pressure curve. Moreover, these peaks, which are significantly higher than the quasi-static pressure, mostly occur within 1 ms, and this observation serves as the basis for determining the end time of energy release. In reality, the combustion of detonation products is a highly complex process, and its reaction time and reaction rate are difficult to measure experimentally or derive theoretically. To justify the energy release time interval chosen in this study, the authors will further explore the influence of energy release history on pressure.

According to the way energy release history is defined in AUTODYN, the energy release history can be represented by the following equation:

$$Q_{ab}(t) = Q_{ab}(t_1) \cdot \left( \frac{t-t_0}{t_1-t_0} \right)^n \quad (15)$$

where  $Q_{ab}(t_1)$  is the energy release value corresponding to the end time of energy release and is also the maximum energy release value. In AUTODYN, the energy release between the two time points is linear by default, i. e.,  $n=1$ . In this aspect, the authors started by investigating the influence of the energy release time, namely, keeping  $n=1$  and adjusting  $t_1$ . Three  $t_1$  values were chosen for comparison. When  $t_1$  is 1, 2, and 3 ms, the corresponding curves of energy release history are shown in Fig. 9(a). Taking the charge 7.50 g for example, numerical simulations are performed by adding additional energy according to the curves of

energy release history shown in Fig. 9(a). The curves of the pressure at measurement point P1 are shown in Fig. 9(b). A comparison of the results in the two figures reveals that when the energy release value is fixed, a shorter energy release time leads to a higher peak pressure of the reflected shock wave and a slightly shorter time to reach the peak pressure. However, changing the energy release time does not alter the final result of the quasi-static pressure.

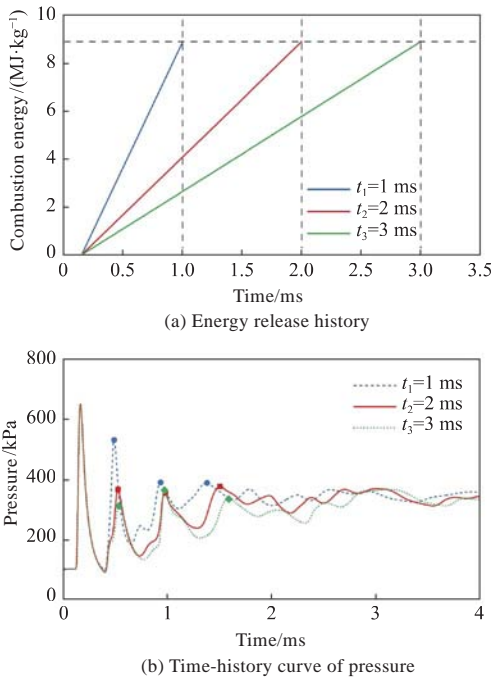


Fig. 9 Influence of energy release time on pressure

Different energy release rates can be achieved by keeping  $t_1 = 2$  ms while changing  $n$ . When  $n$  is set to 1/3, 1, and 3, the corresponding curves of the energy release history are shown in Fig. 10(a). Specifically,  $n=1$  suggests a constant energy release rate;  $n > 1$  indicates a fast-to-slow energy release process;  $n < 1$  signifies a slow-to-fast energy release process. As mentioned earlier, the energy release between two points of time is at a constant rate by default in AUTODYN. To achieve the three energy release modes shown in Fig. 10(a), the authors needed to restart the calculation multiple times to add additional energy piecewise during the simulation. The curves of the pressure at measurement point P1 in the case of a charge of 7.50 g are shown in Fig. 10(b). Clearly, a smaller  $n$  corresponds to a higher peak pressure of the reflected shock wave and a slightly shorter time to reach the peak pressure. However, the final result of the quasi-static pressure remains unchanged.

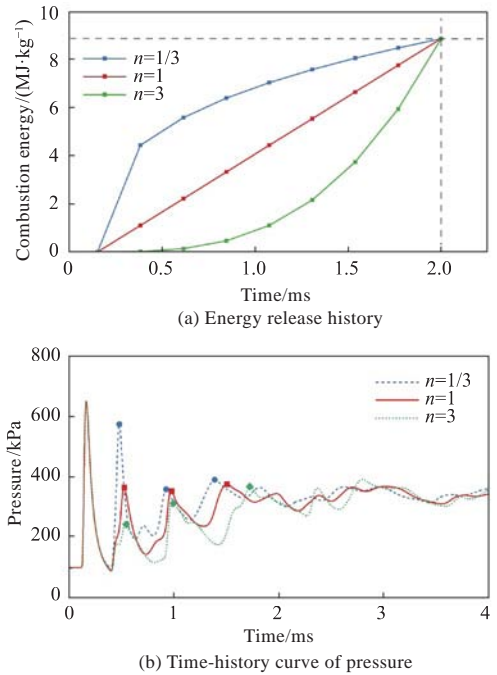


Fig. 10 Influence of energy release rate on pressure

As shown in Fig. 11, the comparison of simulation results with experimental results reveals that the curves of the shock wave pressure corresponding to two energy release modes, namely,  $t_1 = 1$  ms,  $n = 1$ , and  $t_1 = 2$  ms,  $n = 1/3$ , match well with the experimental data. Moreover, the difference between these two groups of simulation results ( $t_1 = 1$  ms,  $n = 1$  and  $t_1 = 2$  ms,  $n = 1/3$ ) is minimal. In spite of different energy release time, these two energy release modes have similar energy release rates within the range of 0 to 0.5 ms according to Figs. 9(a) and 10(a). As a result, their final pressure is also close to each other. Furthermore, the energy release rate in the initial stage (0 to 0.5 ms) plays a dominant role in determining the pressure of the reflected shock wave. Specifically, a faster energy release rate in the initial stage results in higher peak pressure of the reflected shock wave.

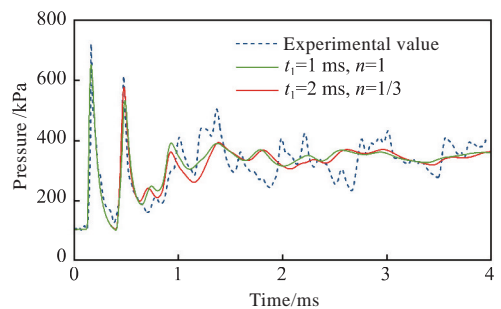


Fig. 11 Comparison among time-history curves of simulation and experimental results of pressure

## 5 Conclusions

An afterburning effect of detonation products can be observed when explosives with negative oxygen balance are detonated in confined spaces. Three calculation methods were summarized to determine the combustion energy released per unit mass of the explosive corresponding to different charge-to-volume ratios. Using the combustion energy values calculated by these three methods as input parameters, the authors conducted simulation calculations under five charge conditions. The following conclusions were drawn from the comparative analysis:

1) The comparison of the experimental results obtained in an air environment with those reached in a helium environment reveals that the combustion energy released per unit mass of the explosive varies significantly under different charge-to-volume ratios. Therefore, the combustion energy corresponding to different charge-to-volume ratios needs to be calculated separately.

2) Among the three calculation methods for combustion energy, Method 1 calculates combustion energy on the basis of chemical reaction analysis and yields theoretical values that are noticeably higher than the actual values but serve as the upper limits. Method 2 is based on energy conservation, and its accuracy depends on the adiabatic index of the post-explosion mixed gases. Method 3 is based on the isentropic process assumption, and the error in the simulation results corresponding to the combustion energy calculated by this method stabilizes in the range of 4% to 7%.

3) The combustion energy release history affects the pressure of reflected shock waves but does not change the final quasi-static pressure. Moreover, a faster energy release rate in the initial stage leads to higher peak pressure of reflected shock waves. Nevertheless, this study only provides a preliminary investigation into the effect of energy release history on the history of the shock wave pressure. Further research is expected to explore the enhancement effects of the combustion of detonation products on the pressure of the reflected shock waves.

## References

- [1] WU W G, KONG X S. Numerical simulation and experiment on damage and protection of warship structures under blast loading [M]. Beijing: Science Press, 2019:1–3 (in Chinese).
- [2] HU H W, SONG P, ZHAO S X, et al. Progress in explosion in confined space [J]. Chinese Journal of Energetic Materials, 2013, 21(4): 539–546 (in Chinese).
- [3] ORNELLAS D L. Calorimetric determinations of the heat and products of detonation for explosives: October 1961 to April 1982 [R]. Berkeley: Lawrence Livermore Laboratory, 1982.
- [4] WOLAŃSKI P, GUT Z, TRZCIŃSKI W A, et al. Visualization of turbulent combustion of TNT detonation products in a steel vessel [J]. Shock Waves, 2000, 10(2): 127–136.
- [5] WANG D W, ZHANG D Z, LI Y, et al. Experiment investigation on quasi-static pressure in explosion containment vessels [J]. Acta Armamentarii, 2012, 33(12): 1493–1497 (in Chinese).
- [6] JIN P G, GUO W, WANG J L, et al. Explosion pressure characteristics of TNT under closed condition [J]. Chinese Journal of Explosives & Propellants, 2013, 36(3): 39–41 (in Chinese).
- [7] ZHANG Y L, SU J J, LI Z R, et al. Quasi-static pressure characteristic of TNT's internal explosion [J]. Explosion and Shock Waves, 2018, 38(6): 1429–1434 (in Chinese).
- [8] KONG X S, KUANG Z, ZHENG C, et al. Experimental study of afterburning enhancement effect for blast load in confined compartment space [J]. Acta Armamentarii, 2020, 41(1): 75–85 (in Chinese).
- [9] EDRI I, FELDGUN V R, KARINSKI Y S, et al. Afterburning aspects in an internal TNT explosion [J]. International Journal of Protective Structures, 2013, 4(1): 97–116.
- [10] FELDGUN V R, KARINSKI Y S, EDRI I, et al. Prediction of the quasi-static pressure in confined and partially confined explosions and its application to blast response simulation of flexible structures [J]. International Journal of Impact Engineering, 2016, 90: 46–60.
- [11] ZHONG W, TIAN Z. Calculation of quasi-static pressures for confined explosions considering chemical reactions under isobaric assumption [J]. Explosion and Shock Waves, 2013, 33(4): 375–380 (in Chinese).
- [12] XU W Z, WU W G. Study on theoretical calculation of quasi-static pressure for explosion in confined space [J]. Chinese Journal of Ship Research, 2019, 14(5): 124–130 (in Chinese).
- [13] LI Y, ZHANG L, DU Z P, et al. Theoretical and experimental study on formation of quasi-static pressure in internal blast [J]. Shipbuilding of China, 2020, 61(2): 28–34 (in Chinese).
- [14] KUHL A L, BELL J B, BECKNER V E, et al. Gasdynamic model of turbulent combustion in TNT explosions [J]. Proceedings of the Combustion Institute, 2011, 33(2): 2177–2185.
- [15] TOGASHI F, BAUM J D, MESTREAU E, et al. Numerical simulation of long-duration blast wave evolution in confined facilities [J]. Shock Waves, 2010, 20(5): 409–424.

- [16] BALAKRISHNAN K, GENIN F, NANCE D V, et al. Numerical study of blast characteristics from detonation of homogeneous explosives [J]. Shock Waves, 2010,20(2): 147-162.
- [17] DONAHUE L, ZHANG F, RIPLEY R C. Numerical models for afterburning of TNT detonation products in air [J]. Shock Waves, 2013, 23(6): 559-573.
- [18] KIM C K, LAI M C, ZHANG Z C, et al. Modeling and numerical simulation of afterburning of thermobaric explosives in a closed chamber [J]. International Journal of Precision Engineering and Manufacturing, 2017, 18(7): 979-986.
- [19] XU W Z, WU W G. Study on numerical calculation of explosion field in confined space considering afterburning effects [J]. Chinese Journal of Energetic Materials, 2019, 27(8): 661-670 (in Chinese).
- [20] XU W Z, WU W G. Afterburning effect on blast load in confined space [J]. Chinese Journal of Ship Research, 2019, 14(1):52-58 (in Chinese).
- [21] XU W Z, WU W G, KUANG Z. Method for theoretically predicting time history of afterburning reaction rate of internal explosion and determining energy release constant [J]. Chinese Journal of Ship Research, 2019, 14(4): 22-29 (in Chinese).
- [22] LI G, LU F Y, LI X Y, et al. Numerical simulation and experimental verification on the energy release law of thermostatic explosive based on gas-solid two-phase reaction flow [J]. Chinese Journal of Explosives & Propellants, 2021, 44(2): 195-204 (in Chinese).
- [23] XIN C L, XU G G, LIU K Z, et al. Numerical simulation of TNT explosion with post-detonation burning effect in air [J]. Chinese Journal of Energetic Materials, 2008, 16(2):160-163 (in Chinese).
- [24] EDRI I, FELDGUN V R, KARINSKI Y S, et al. On blast pressure analysis due to a partially confined explosion: III. Afterburning effect [J]. International Journal of Protective Structures, 2012, 3(3): 311-331.
- [25] CAO W, HE Z, CHEN W. Experimental study and numerical simulation of the afterburning of TNT by underwater explosion method [J]. Shock Waves, 2014, 24(6): 619-624.
- [26] HERNANDEZ F, HAO H, ABDEL-JAWAD M. Additional afterburning energy value to simulate fully confined trinitrotoluene explosions [J]. International Journal of Protective Structures, 2016, 7(2): 232-264.
- [27] KONG X S, XU J B, XU W Z, et al. Numerical study of influence of afterburning effect on blast load in confined cabin [J]. Acta Armamentarii, 2019, 40(4): 799-806 (in Chinese).
- [28] UFC-3-340-02 Structures to resist the effect of accidental explosions [S]. U. S. Army Corps of Engineers, Naval Facilities Engineering Command, Air Force Civil Engineer Support Agency, 2014.
- [29] SONG P, YANG K, LIANG A D, et al. Difference analysis on JWL-EOS and energy release of different TNT charge [J]. Chinese Journal of Explosives & Propellants, 2013, 36(2): 42-45 (in Chinese).
- [30] LUO Y M, SHEN F, JIANG Q L, et al. Driving performance and JWL EOS of DNTF charge with two densities [J]. Chinese Journal of Explosives & Propellants, 2021, 44(2): 175-180 (in Chinese).

## 舱室内爆载荷燃烧增强效应试验及仿真研究

岳学森<sup>1</sup>, 周沪<sup>1</sup>, 孔祥韶<sup>\*2</sup>, 郑成<sup>2</sup>, 吴卫国<sup>2</sup>

1 武汉理工大学 船海与能源动力工程学院, 湖北 武汉 430063

2 武汉理工大学 绿色智能江海直达船舶与邮轮游艇研究中心, 湖北 武汉 430063

**摘要:** [目的] TNT炸药在密闭空间中发生爆炸时,其爆轰产物的燃烧效应不可忽视,为准确分析TNT炸药在密闭空间中的爆炸载荷,需要探究爆轰产物燃烧释放的能量与药量体积比的关系。[方法] 首先开展5种不同质量的TNT分别在空气和氮气环境密闭空间中的爆炸试验,然后基于化学反应分析、能量守恒、等熵假设3种不同的方法计算5种不同药量体积比对应的爆轰产物燃烧能量,并基于有限元分析软件ANSYS/AUTODYN开展考虑燃烧效应的密闭空间内爆炸数值计算。[结果] 准静态压力仿真结果与试验结果的对比表明:3种方法中,通过化学反应计算得到的燃烧能量理论值可作为上限值,能量守恒法的准确性依赖爆炸后混合气体的绝热指数,等熵假设法仿真值与试验值误差稳定在4%~7%之间;不同的燃烧能量释放历程会影响反射冲击波压力,但不改变最终的准静态压力。[结论] 研究结果可为舰船抗爆结构设计及毁伤评估提供更精确的输入载荷。

**关键词:** 内爆载荷; 燃烧效应; 能量释放; 准静态压力